EURASIP Journal on
Wireless Communications and Networking
a SpringerOpen Journal

RESEARCH   **Open Access**

A novel link switching scheme using pre-scanning and RSS prediction in visible light communication networks

Tuan Nguyen[1], Mostafa Zaman Chowdhury[2] and Yeong Min Jang[1*]

Abstract

Visible light communication (VLC) is gaining increasing attention and is considered as a promising technology for future wireless indoor communications. Because movable users expect a seamless connectivity experience when switching among transmitters (i.e., VLC access points) in the VLC system, fast link switching operations must be supported by the networks. This paper presents a novel hard link switching scheme for VLC networks with the use of pre-scanning and received signal strength (RSS) prediction. Our proposed scheme achieves the advantages of both conventional hard and soft link switching schemes without changing device hardware or the IEEE 802.15.7 medium access control (MAC) protocol. To help compare our proposed scheme with conventional hard and soft link switching schemes, the signal-to-interference-plus-noise ratio (SINR), the outage probability regarding the link switching situation, and the queuing models for link switching schemes are taken into account. Simulation and numerical results validate that our proposed scheme outperforms conventional hard and soft link switching schemes.

Keywords: Link switching; Handover; Pre-scanning; VLC; Visible light communication; RSS prediction; Outage probability

1. Introduction

Because the requirements for wireless data communication continually increase, the radio frequency spectrum is becoming congested. Hence, quests for alternative communication technologies have been carried out increasingly around the world. In recent years, visible light communication (VLC) has attracted the attention of researchers and has been considered as a promising technology for future wireless communications, especially indoor communications. VLC refers to short-range optical wireless communication using the visible light spectrum from 380 to 780 nm [1]. Compared to radio frequency (RF) technologies, VLC has many advantageous features such as high-speed transmission, visibility, high security, harmlessness to the human body, high tolerance to humidity, ubiquity, and an unlicensed frequency spectrum [2-4]. In 2011, VLC technology was standardized by the IEEE organization in the IEEE 802.15.7 specification [5].

Link switching, commonly known as handover in other wireless communication technologies, is an essential issue that deals with the mobility of end users (the term 'link switching' is used in the IEEE 802.15.7 standard instead of 'handover'). It guarantees seamless connectivity or improves the quality of service (QoS). In first-generation cellular systems, such as the Advanced Mobile Phone System (AMPS) [6], or second-generation systems such as the Global System for Mobile Communication (GSM) [7] and Personal Access Communications System (PACS) [8], a hard handover is deployed. In the hard handover, the old radio link is broken before a new radio link is established, and a user device only connects to one base station at any given time. In third-generation systems, which are mainly based on code-division multiple-access (CDMA) technology, the soft handover concept is introduced [9]. In a soft handover, a user device can communicate with the system using multiple radio links through different base stations simultaneously. Compared to the conventional hard handover, a soft handover produces a smoother transmission and reduces the so-called 'ping-pong' effect [10-12], but it has the disadvantages of implementation complexity and extra resource consumption.

* Correspondence: yjang@kookmin.ac.kr
[1]Department of Electronics Engineering, Kookmin University, Seoul 136-702, South Korea
Full list of author information is available at the end of the article

Springer

Handover is a classic research topic. A larger number of papers have been presented to cope with problems in handover. Some popular problems include the handover delay [13-16], the ping-pong effect, the handover procedure in heterogeneous networks [17-20], and the handover failure rate [21-24]. However, as far as we know, there are not many papers studying link switching in VLC networks. In [25], a handover mechanism between Wi-Fi and VLC is proposed to dynamically distribute resources to optimize system throughput and to avoid service disconnections. The work in [26] investigates how handover techniques can be applied in VLC networks in which user connectivity switches from one lighting cell to another. In [27], based on minimum QoS requirements of traffic, a flexible resource allocation scheme is proposed to support link switching in VLC networks.

In this paper, we propose a novel hard link switching scheme for VLC networks, using a pre-scanning method and a received signal strength (RSS) prediction scheme, to overcome some drawbacks of conventional hard and soft link switching schemes. Our proposed scheme efficiently reduces the link switching delay compared to conventional hard link switching scheme as well as reduces the unnecessary the link switching ratio and the outage probability compared to conventional hard and soft link switching schemes. To utilize our proposed scheme, there is no need to change the hardware of user devices as in the case of a conventional soft link switching scheme. Through queuing analysis, our proposed scheme exhibits lower link switching call dropping probability and new call blocking probability compared to a conventional soft link switching scheme. The main contributions of the work in this paper are the following:

1) A novel pre-scanning method, which suits the IEEE 802.15.7 medium access control (MAC) operation, is proposed to eliminate the impact of the scanning process on the link switching delay.
2) A new serving transmitter selection method, using an RSS prediction method, in the link switching decision phase is proposed. This approach can help reduce the unnecessary link switching ratio.
3) An in-depth study of the signal-to-interference-plus-noise ratio (SINR) and outage probability regarding the link switching situation in a VLC environment.

The rest of this paper is organized as follows: Section 2 describes the system model of VLC networks including the optical channel model, IEEE 802.15.7 MAC, and link switching fundamentals. Section 3 presents our proposed fast link switching scheme with a theoretical analysis of SINR, the outage probability, and a queuing model.

Section 4 evaluates the performance of our proposed schemes in terms of several important metrics and in comparison with conventional hard and soft link switching schemes. Finally, Section 5 concludes our work.

2. VLC system model
In the IEEE 802.15.7 standard, there are three basic devices: a user device, a transmitter, and a single central controller called the coordinator. User devices and transmitters use visible light links to transmit or receive data. Transmitters of a VLC network are managed by a coordinator [5]. The IEEE 802.15.7 architecture is defined in terms of the number of layers and sublayers in order to simplify the standard. A VLC device is composed of a PHY layer, which contains the light transceiver along with its low-level control mechanism, and a MAC sublayer that provides access to the physical channel for all types of transfers. In this section, we represent the optical channel model, the IEEE 802.15.7 MAC protocol, and the link switching fundamentals.

2.1. Optical channel model
There are two types of links that can be used in a VLC system: line-of-sight (LOS) and non-line-of-sight (NLOS), as shown in Figure 1. To achieve a high data rate as well as to minimize path loss and to maximize the power efficiency, LOS links should be used. The optical channel gain is expressed as

$$P_r = H(0)P_t, \tag{1}$$

where P_t is the transmitted power, P_r is the received power, and $H(0)$ is the channel DC gain.

In the case of LOS links, the channel DC gain is defined as

$$H_{LOS}(0) = \begin{cases} \dfrac{(m+1)A}{2\pi d^2} \cos^m(\phi) T_s(\psi) g(\psi) \cos(\psi) & 0 \leq \psi \leq \psi_c \\ 0 & \text{elsewhere} \end{cases}, \tag{2}$$

where m is the order of the Lambertian emission, A is the photodetector area, d is the distance between the transmitter and user device, φ is the angle of irradiance, ψ is the angle of incidence, $T_s(\psi)$ is the signal transmission coefficient of an optical filter, $g(\psi)$ is the gain of an optical concentrator, and ψ_c is the receiver field of view (FOV).

The order of the Lambertian emission, m, is found from the following equation:

$$m = -\frac{\ln 2}{\ln\left(\cos\phi_{1/2}\right)}, \tag{3}$$

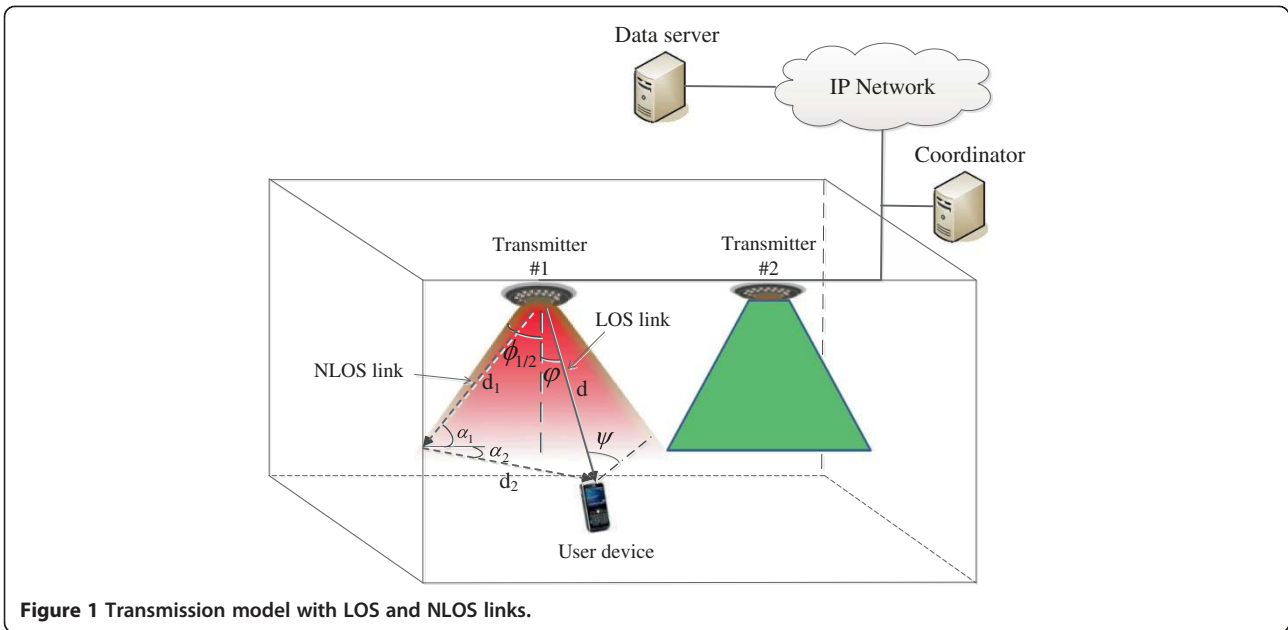where $\phi_{1/2}$ is the transmitter semi-angle at half power.

Figure 1 Transmission model with LOS and NLOS links.

The gain of an optical concentrator, $g(\psi)$, is found from the following equation:

$$g(\psi) = \begin{cases} \dfrac{\alpha^2}{\sin^2(\psi_c)} & 0 \le \psi \le \psi_c, \\ 0 & \text{elsewhere} \end{cases} \quad (4)$$

where α is the refractive index of the optical concentrator.

In the case of NLOS links, the channel DC gain on the first reflection is

$$H_{NLOS}(0) = \begin{cases} \dfrac{(m+1)A}{2\pi d_1^2 d_2^2} \Lambda A_{\text{wall}} \cos^m(\phi)\cos(\alpha_1)\cos(\alpha_2)T_s(\psi)g(\psi)\cos(\psi) \\ 0 \end{cases}$$
$$\begin{matrix} 0 \le \psi \le \psi_c \\ \text{elsewhere} \end{matrix},$$

$$(5)$$

where Λ is the reflectance factor, A_{wall} is the reflective area of a small region, α_1 is the angle of irradiance to a reflective point, α_2 is the angle of irradiance to the receiver, d_1 is the distance between the transmitter and the reflective point, and d_2 is the distance between the reflective point and the user device.

In this paper, in order to simplify the theoretical analysis as well as the simulation, we assume that the channels of the VLC system are Rician channels in which LOS links are the strong dominant components.

2.2. IEEE 802.15.7 MAC protocol

The IEEE 802.15.7 MAC protocol [5], as well as the IEEE 802.15.4 MAC protocol [28], supports both beacon-enabled mode and non-beacon-enabled mode. In the non-beacon-enabled mode, it is a simple unslotted random access mechanism, with or without carrier sense multiple-access with collision avoidance (CSMA/CA). Because most of the unique features of IEEE 802.15.7 are in the beacon-enabled mode, we will focus on describing it.

Figure 2 shows the superframe structure adopted by the IEEE 802.15.7 beacon-enabled mode. A superframe is bounded by the transmission of beacon frames and can have an active portion and an inactive portion. The duration of a superframe, also called the beacon interval (BI), is described as

$$BI = aBaseSuperframeDuration \times 2^{BO}, \quad 0 \le BO \le 14,$$
$$(6)$$

where BO is the value of *macBeaconOrder* that describes the interval in which the coordinator will transmit its beacon frame and *aBaseSuperframeDuration* describes the number of optical clocks forming a superframe when the superframe order is equal to 0. If $BO = 15$, the coordinator will not transmit beacon frames except when it is requested to do so.

During the inactive portion, a VLC device may enter a low-power mode, such as idle mode or sleep mode, to save power. The active portion is divided into 16 equal time slots, as in the IEEE 802.15.7 standard, and is composed of three parts: a beacon, a contention access period (CAP), and a contention free period (CFP). If a user device is allocated to a specific time slot, it can use the whole channel within that time slot duration. The beacon is transmitted, without the use of any random access, at the start of slot 0. The CAP starts immediately following the beacon and completes before the beginning of the CFP on
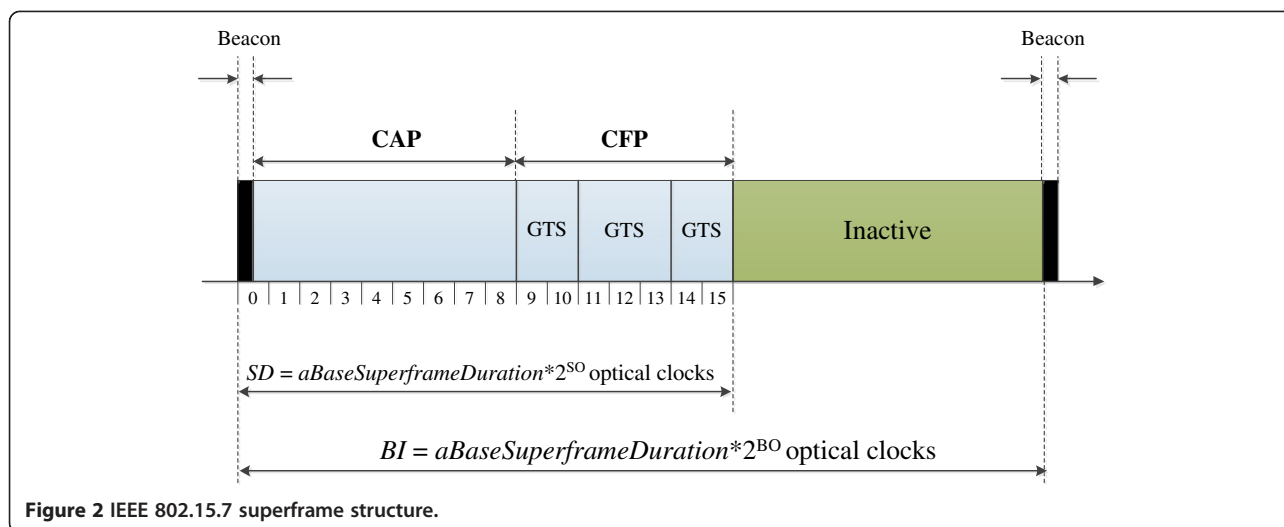
Figure 2 IEEE 802.15.7 superframe structure.

a superframe slot boundary. The duration of the active portion, denoted as SD, is described as

$$SD = aBaseSuperframeDuration \times 2^{SO}, \quad 0 \leq SO \leq 14,$$

(7)

where SO is the value of *macSuperframeOrder* that describes the length of the active portion of a superframe. If $SO = 15$, the superframe will not remain after the beacon.

In CAP, devices use a slotted CSMA/CA mechanism to access the channel. The CFP is dedicated to support time-critical data transfers generated by the applications that require specific data bandwidth or low latency. In CFP, data are transmitted in guaranteed time slots (GTS). A GTS can be allocated to an integer number of time slots, and GTSs are allocated on a first-come-first-served (FCFS) basis. Each GTS is reallocated when it is no longer required, or when it has not been used for a specified duration.

### 2.3. Link switching fundamentals

To support the mobility of user devices, the IEEE 802.15.7 standard presents the usage of cell design and PHY switch [5]. These procedures may be efficiently applicable within a VLC network where user devices do not need to change the network information, such as network ID, and the MAC operation during their movements in order to maintain the data transmission. Besides, in using these procedures, outage may happen because there is no guarantee on the quality of signals (for example, these procedures do not cope with the situation that the RSS of a user device may drop seriously when the user device moves to/move out of the boundary area of a cell). Generally, to support the mobility of user devices within a VLC network as well as among VLC networks, link switching (i.e., handover) is a comprehensive solution.

Link switching refers to the process of transferring an ongoing data session (messages, voice calls, video calls, etc.) of a device from one transmitter to another. Link switching is a significant issue in terms of maintaining seamless connectivity or improving QoS. In a homogeneous system, a link switching technique can be divided into two types: hard link switching and soft link switching. Figure 3 shows the basic call flow of a conventional hard link switching technique with the VLC system depicted in Figure 1. When the received signal strength is under a threshold level, the user device sends the measurement report to its current serving transmitter, i.e., Transmitter #1 (steps 1 and 2). After that, the user device starts scanning neighboring transmitters, by switching among all channels, to find the best one based on some criteria, such as RSS, resource availability, and others (steps 3 and 4). The scanning time of a user device on a channel, denoted as $T_{\text{chann\_scan}}$, is defined as

$$T_{\text{chann}_{\text{scan}}} = aBaseSuperframeDuration \times (2^n + 1)$$

(8)

where n is the value of the *ScanDuration* parameter $(0 \leq n \leq 14)$.

After finding the best neighboring transmitter, the user device needs to disconnect from its current serving transmitter (steps 5 to 7). To disconnect the user device from its serving transmitter, the coordinator releases the resources of Transmitter #1 that are used for the user device. The user device starts connecting to the selected neighboring transmitter by sending a link switching request (step 8). The coordinator performs call admission control and radio resource control to check if the call is accepted or not (step 9). After that, the coordinator responses to the link switching request of the user device (step 10). Then, the user device starts, one by one, the association process and

Figure 3 Conventional hard link switching call flow.
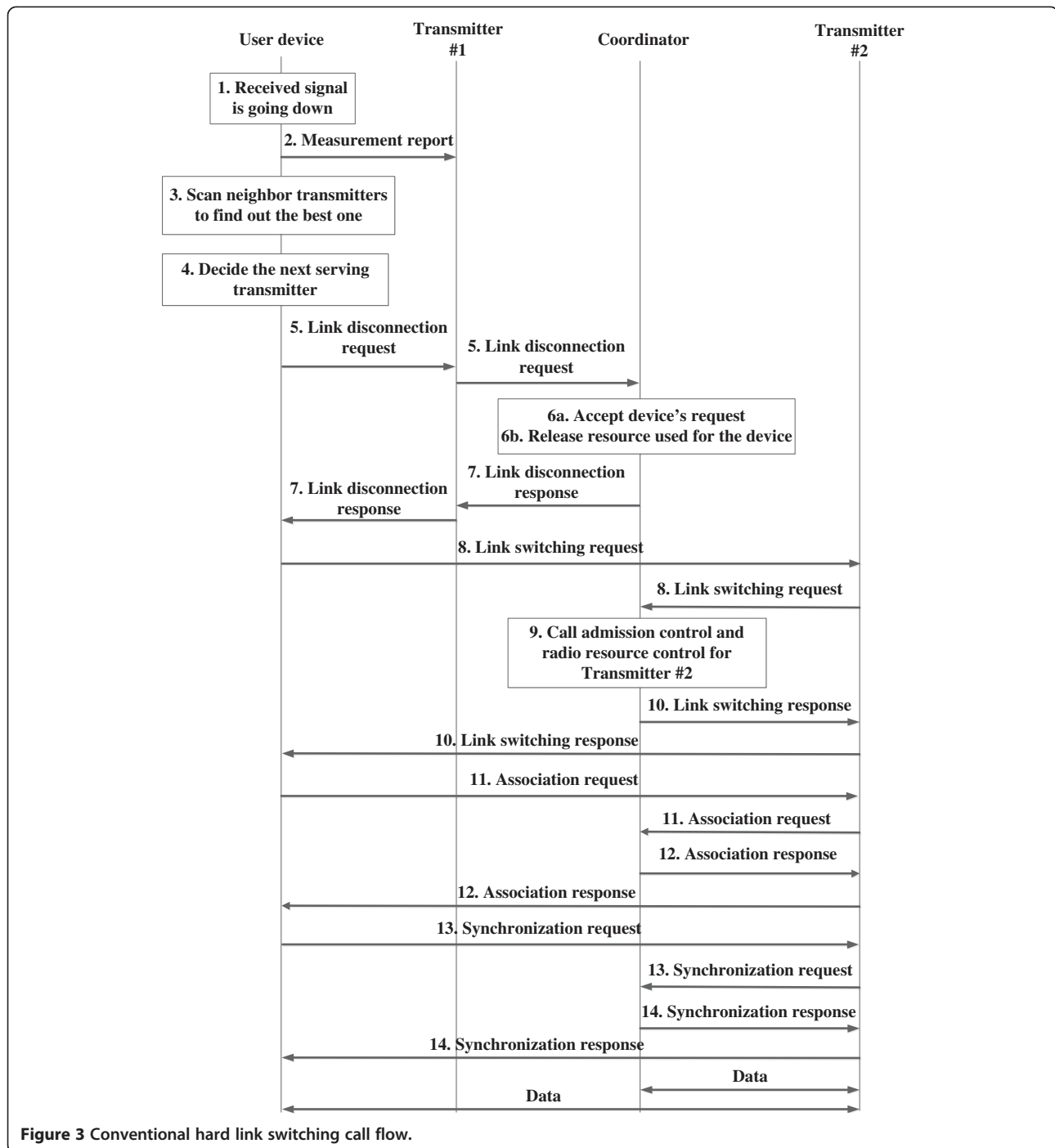
synchronization process with the selected neighboring transmitter, i.e., Transmitter #2 (steps 11 to 14). The user device and the selected neighboring transmitter exchange information such as the network ID, beacon interval, the addresses of the devices, and the channel identification. Finally, the data are sent to the user device through Transmitter #2.

During a hard link switching procedure, user devices cannot receive the signal from the serving transmitter, which leads to a data interruption problem and then QoS degradation. Thus, the process duration of a hard link switching scheme (i.e., link switching delay), which mainly originates from the scanning period, is an important problem in terms of guaranteeing a seamless data transmission. This problem can be solved effectively in soft link switching. In soft link switching, a user device can simultaneously communicate with two or more transmitters, including its current serving transmitter. The link between the

user device and its current serving transmitter is disconnected only after it has successfully connected to the target transmitter.

The main advantage of soft link switching over hard link switching is a better guarantee in data transmission, which originates from the significantly smaller link switching delay. However, to utilize soft link switching, the hardware of user devices must be more complex and expensive compared to that of hard link switching to be able to receive signals from many transmitters simultaneously. Another problem of the soft link switching technique is the use of several channels to only support a single user device, which results in a waste of resources, an increase in the volume of data traffic, and an increase in downlink interference.

A link switching may be interrupted in case the user device or the transmitter does not receive the link switching-related signals due to certain factors (such as interference) or the available resources of the selected neighboring transmitter are not enough to be allocated to the user device. To solve these problems, the IEEE 802.15.7 standard presents the fast link recovery and multiple-channel resource assignment procedures [5]. The details of these procedures are beyond the scope of this paper.

3. Proposed hard link switching scheme

In this section, we represent our proposed link switching scheme for a VLC system exploiting the operation of the IEEE 802.15.7 MAC protocol. By using our scheme, we can eliminate the scanning period, which has the largest impact on the link switching delay, in a link switching procedure. Additionally, our proposed scheme does not require a change in IEEE 802.15.7 MAC operation and the hardware of user devices as in the case of a soft link switching technique. The theoretical analysis of the proposed scheme is also presented in this Section.

3.1. Proposed link switching scheme

As mentioned before, in the IEEE 802.15.7 MAC protocol, during the inactive portion, VLC devices may enter a low-power mode, such as idle or sleep mode. Our proposed scheme utilizes this period for user devices to scan channels, associate, and synchronize with a target transmitter, respectively.

The main steps of our proposed scheme are depicted in Figure 4. During its operation in a VLC system, after having received a signal from its current serving transmitter, a user device measures the received signal strength, denoted as $P_{r,curr}$. The value of $P_{r,curr}$ is compared to three thresholds, denoted as Scan_thr, Assoc_thr, and LS_thr (Scan_thr > Assoc_thr > LS_thr), to determine the next process precisely. These three thresholds divide the proposed link switching procedure into three periods

called pre-scanning, pre-association, and the final link switching decision.

3.1.1. Pre-scanning period
A user device initiates the pre-scanning process if the following criterion is met:

$$Assoc\_thr \leq P_{r,curr} < Scan\_thr \qquad (9)$$

In the pre-scanning period, firstly, the user device scans all the channels, using either active scanning or passive scanning, to find the neighboring transmitters. To achieve this task and in order not to interrupt data reception from the current serving transmitter of the user device, the scanning time of all channels should be shorter than the duration of the inactive portion of the superframe. To fulfill this requirement, based on Equations (6) to (8), the value of the *ScanDuration* parameter, n, needs to satisfy the following equation:

$$2^{BO} - 2^{SO} > k(2^n + 1), \qquad (10)$$

where k is the number of channels in a VLC system. In the IEEE 802.15.7 standard, the value of k is 7.

After the scanning process, the user device saves all the values of the RSSs measured from the signals of neighboring transmitters. Finally, the user device returns to receive data following the IEEE 802.15.7 MAC superframe operation.

The pre-scanning procedure may be initiated if the current RSS of the user device satisfies Equation (9). This work has two purposes:

– All the saved values of RSSs from the signals of neighboring transmitters will be used in the pre-association process for determining the best neighboring transmitter. The detailed steps are explained in the next section.

– During the scanning process, because of several factors, such as interference, noise, channel access failure, transmission speed, and short scanning time on channels, a user device may not receive beacon signals from a (or some) neighboring transmitter(s). Thus, multiple pre-scannings help a user device to eliminate this problem; since then, the scanning result is improved.

In reality, the movement of user devices is random. This problem results in the random variation of the RSS. In some cases, after a duration in which the value of $P_{r,curr}$ is below the Scan_thr threshold, $P_{r,curr}$ then becomes higher than Scan_thr, and is maintained for a sufficiently long duration (for example, when a user device first arrives in the boundary area of its current serving transmitter and then returns towards the current serving transmitter, its $P_{r,curr}$ value may change from a weak value to a strong value). In these cases, the saved RSS values from the signals of neighboring transmitters are not valuable now.
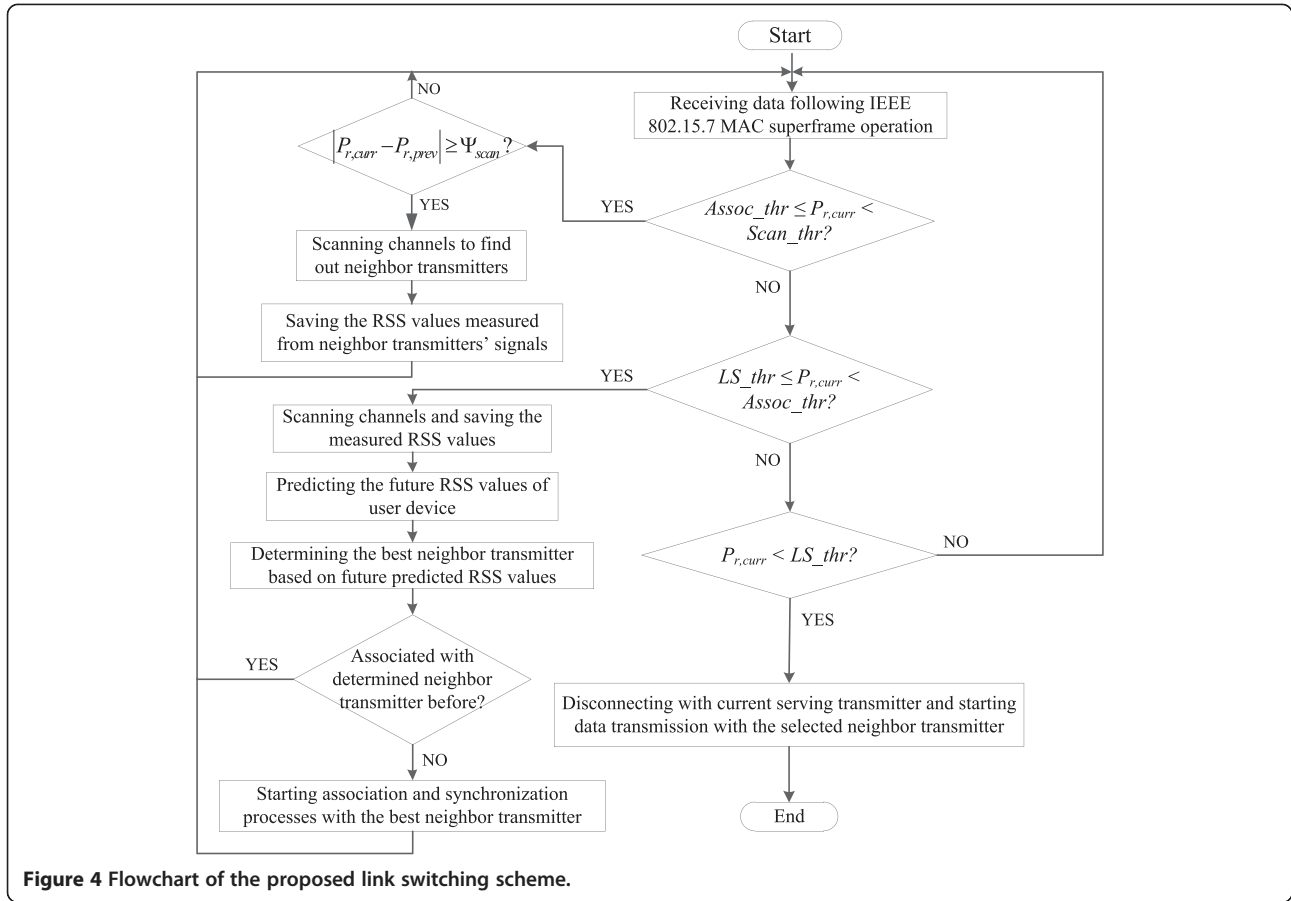
Figure 4 Flowchart of the proposed link switching scheme.

Thus, to reduce the size of the RSS database, all the saved RSS values are removed if the following criterion is met:

$$T_r > \tau, \tag{11}$$

where T_r is the duration, in the number of superframes, in which the value of $P_{r,curr}$ is higher than the value of Scan_thr. τ is a predefined integer threshold ($\tau > 0$).

Additionally, a user device may stay in a certain location, where its value of $P_{r,curr}$ satisfies Equation (9), for a long time, or its movement speed is slow resulting in its RSS value not varying significantly. In these cases, the user device may unnecessarily initiate the scanning process continuously. To avoid this problem, the user device only starts the next scanning process if its current RSS value differs from its previous RSS value by a hysteresis margin Ψ_{scan}:

$$\left| P_{r,curr} - P_{r,prev} \right| \geq \Psi_{scan}. \tag{12}$$

3.1.2. Pre-association period

The second period of our proposed link switching scheme is the pre-association period. A user device starts the pre-association process if the following criterion is met:

$$LS\_thr \leq P_{r,curr} < Assoc\_thr. \tag{13}$$

In the pre-association period, first, the user device starts scanning and then saving RSS values of the signals of neighboring transmitters to obtain their most recent values. After that, the user device needs to determine the best neighboring transmitter, which has the strongest future-predicted signal strength. To achieve the future RSS values of the signals of neighboring transmitters, we use the saved RSS values and apply a prediction method described in [29]. This prediction scheme is validated to achieve a small prediction error and indicate the possibility of implementation. The raw predictive RSS value of neighboring transmitter j in the nth process (n can be understood as the order in the saved RSS data sequence), denoted as $P_{r,raw}(j, t_n)$, is measured by

$$P_{r,raw}(j, t_n) = a_0 t_n^0 + a_1 t_n^1 + a_2 t_n^2 + a_3 t_n^3 + \ldots + a_z t_n^z, \tag{14}$$

where a_i is an unknown coefficient ($0 \leq i \leq z, z \in Z^+$).

The values of the coefficients are obtained from the following polynomials:

$$\begin{cases} a_0\left(\sum_{i=1}^{n}t_i^0\right) + a_1\left(\sum_{i=1}^{n}t_i^1\right) + a_2\left(\sum_{i=1}^{n}t_i^2\right) + a_3\left(\sum_{i=1}^{n}t_i^3\right) + ... + a_z\left(\sum_{i=1}^{n}t_i^z\right) = \sum_{i=1}^{n}t_i^0 P_{\mathrm{r}}(j,t_n) \\ a_0\left(\sum_{i=1}^{n}t_i^1\right) + a_1\left(\sum_{i=1}^{n}t_i^2\right) + a_2\left(\sum_{i=1}^{n}t_i^3\right) + a_3\left(\sum_{i=1}^{n}t_i^4\right) + ... + a_z\left(\sum_{i=1}^{n}t_i^{z+1}\right) = \sum_{i=1}^{n}t_i^1 P_{\mathrm{r}}(j,t_n) \\ \vdots \qquad \vdots \qquad \vdots \qquad \vdots \qquad \vdots \qquad \vdots \\ a_0\left(\sum_{i=1}^{n}t_i^z\right) + a_1\left(\sum_{i=1}^{n}t_i^{z+1}\right) + a_2\left(\sum_{i=1}^{n}t_i^{z+2}\right) + a_3\left(\sum_{i=1}^{n}t_i^{z+3}\right) + ... + a_z\left(\sum_{i=1}^{n}t_i^{2z}\right) = \sum_{i=1}^{n}t_i^z P_{\mathrm{r}}(j,t_n) \end{cases} \tag{15}$$

where $P_{\mathrm{r}}(j, t_n)$ is the saved RSS value in the nth process.

If we consider coefficients as variables, by applying the Gauss elimination method [30] to Equation (15), we calculate all the coefficients as

$$a_i = \frac{1}{A_{i,i}}\left(b_i - \sum_{j=i+1}^{z} A_{i,i}a_j\right), \tag{16}$$

where $A_{i,i}$ and b_i are elements of the augmented coefficient matrix that is generated after several steps of Gauss elimination.

The final predictive RSS value in the $(n + 1)$th process, which is used for determining the best neighboring transmitter, is denoted as $P_{\mathrm{r,pred}}(j, t_{n+1})$ and is calculated as

$$P_{r,pred}(j, t_{n+1}) = P_{r,raw}(j, t_{n+1}) - \sum_{j=1}^{n} P_r(j, t_j) \tag{17}$$

After obtaining the predictive RSS values (i.e., $P_{r,pred}(j, t_{n+1})$) of all neighboring transmitters, the user device starts association and synchronization with the best neighboring transmitter that satisfies the three following criteria:

a) The user device is moving closer to this neighboring transmitter, which is expressed by the following equation:

$$P_{r,pred}(j, t_{n+1}) - P_r(j, t_n) > 0 \tag{18}$$

b) The value of $P_{r,pred}(j, t_{n+1})$ of this neighboring transmitter is higher than the value of LS_thr.
c) Among neighboring transmitters that satisfy criteria (a) and (b), the best neighboring transmitter is the one whose predictive RSS value is highest.

Finally, the user device returns to receive data following the IEEE 802.15.7 MAC superframe operation.

The pre-association procedure may happen several times because the value of $P_{r,curr}$ of a user device may be in the range of [LS_thr;Assoc_thr) in some superframe periods. Thus, to reduce the necessity of performing association and synchronization processes with the same neighboring transmitter, before starting these two processes, if a user device is already associated with the selected neighboring transmitter, it will skip these processes and return to receive data from its current transmitter in the next superframe.

The difference between our proposed scheme and a soft link switching scheme is that, after the pre-association procedure, a user device does not transmit and receive data with the selected neighboring transmitter. It only keeps pieces of information related to that neighboring transmitter, such as the address, beacon interval, channel identification, and network identification, which are used to connect to that transmitter in the final phase of our proposed link switching scheme. This work helps avoid the waste of resources caused by using several channels to support just a single user device.

3.1.3. Final link switching decision
The final period of our proposed scheme is started when the value of $P_{r,curr}$ of a user device is smaller than the LS_thr threshold. At this time, first, the user device disassociates with its current serving transmitter and deletes all the information related to it. Because the user device has already used the resources of this transmitter, it cannot disassociate itself as we explained above. In this case, the user device needs to send a disassociation message to its current serving transmitter so that this transmitter can release resources allocated for the user device to avoid the waste of resources.

Finally, by using information gained in the pre-association period, the user device switches to the channel of the neighboring transmitter, which was selected in the pre-association period, and follows the superframe operation of this transmitter. Now, the selected neighboring transmitter becomes the new serving transmitter of the user device.

3.2. Theoretical analysis

The outage probability is an important metric in wireless communication systems. To maintain the QoS, the RSS, or the SINR needs to be maintained above a certain threshold. In this paper, we focus on analyzing the outage probability with respect to three link switching schemes, which are conventional hard link switching, conventional soft link switching, and our proposed link switching.

3.2.1. SINR calculation

We assume that all transmitters have the same transmitted power. Thus, the inter-cell interference to the connection between a user device and transmitter i at location x, denoted as $\text{ICI}_{x,i}$, is given by

$$\text{ICI}_{x,i} = \sum_{j=1}^{N_t} \beta P_t H(x,j), \tag{19}$$

where N_t is the total number of neighboring transmitters, $H(x, j)$ is the channel DC gain at location x with respect to transmitter j, and β is the detector responsivity.

Let $\text{SNR}_{x,i}$ denote the signal-to-noise ratio of the signal received from transmitter i when the user device is at location x. The value of $\text{SNR}_{x,i}$ is calculated as [31].

$$\text{SNR}_{x,i} = \frac{(\beta P_r(x,i))^2}{\sigma_{total}^2}, \tag{20}$$

where $P_r(x, i)$ is the received power at location x with respect to transmitter i, and σ_{total}^2 is the total variance of the Gaussian noise, which is the sum of contributions from the shot noise and thermal noise:

$$\sigma_{total}^2 = \sigma_{shot}^2 + \sigma_{thermal}^2 \tag{21}$$

Consequently, we have

$$\text{SNR}_{x,i} = \frac{(\beta P_r(x,i))^2}{\sigma_{shot}^2 + \sigma_{thermal}^2} = \frac{(\beta P_t H(x,i))^2}{\sigma_{shot}^2 + \sigma_{thermal}^2} \tag{22}$$

The value of $\text{SINR}_{x,i}$ is expressed as

$$SINR_{x,i} = \frac{(\beta P_t H(x,i))^2}{\text{ICI}_{x,i}^2 + \sigma_{shot}^2 + \sigma_{thermal}^2} \tag{23}$$

In a VLC network, at a certain time, there is only one user device using the channel of a transmitter. Thus, intra-cell interference does not occur, and we do not take into account intra-cell interference in this paper.

3.2.2. Outage probability

The outage probability at a location is defined as the probability that the SINR value at that location is less than a specified threshold Out_thr. It is calculated as

$$
\begin{aligned}
R_{\text{out},x}(i) &= R\big[SINR_{x,i} < Out\_thr\big] \\
&= \int_{-\infty}^{\infty} R[SINR_{x,i} < Out\_thr | G_\sigma = G_o].R[G_\sigma = G_o]dG_o \\
&= \int_{-\infty}^{\infty} R[SINR_{x,i} < Out\_thr | G_\sigma = G_o].\frac{1}{\sqrt{2\pi}\sigma}e^{-\frac{G_o^2}{2\sigma^2}}dG_o
\end{aligned}
\tag{24}
$$

where $R_{\text{out},x}(i)$ is the outage probability at location x with respect to transmitter i.

Substituting Equation (23) into Equation (24), we have

$$
\begin{aligned}
R_{\text{out},x}(i) &= \int_{-\infty}^{\infty} R\left[\frac{(\beta P_t H(x,i))^2}{\text{ICI}_{x,i}^2 + \sigma_{shot}^2 + \sigma_{thermal}^2} < Out\_thr | G_\sigma = G_o\right] \\
&\quad \times \frac{1}{\sqrt{2\pi}\sigma}e^{-\frac{G_o^2}{2\sigma^2}}dG_o \\
&= \int_{-\infty}^{\infty} R\left[H(x,i) < \frac{\sqrt{Out\_thr\left(\text{ICI}_{x,i}^2 + \sigma_{shot}^2 + \sigma_{thermal}^2\right)}}{\beta P_t} | G_\sigma = G_o\right] \\
&\quad \times \frac{1}{\sqrt{2\pi}\sigma}e^{-\frac{G_o^2}{2\sigma^2}}dG_o
\end{aligned}
\tag{25}
$$

The path loss model of the VLC system is given as [32]

$$
\begin{aligned}
N(x,i) &= 10\log\left(\frac{P_t}{E(d_{ref}(x,i))A_0}\right) - 10\log\left(\frac{A}{A_0}\right) \\
&\quad + 10p\log\left(\frac{d(x,i)}{d_{ref}(x,i)}\right) + G_\sigma,
\end{aligned}
\tag{26}
$$

where $N(x, i)$ is the path loss at location x with respect to transmitter i, $d(x,i)$ is the distance between the user device and transmitter i at location x, $d_{\text{ref}}(x, i)$ is the reference distance, $E(d_{\text{ref}}(x,i))$ is the irradiance at the reference distance $d_{\text{ref}}(x, i)$, A_0 is the reference photodetector area, G_σ is a zero-mean Gaussian distributed random variable with standard deviation σ, and p is the path loss exponent.

Because $N(x, i)$ is a random variable with a normal distribution, so is the received power $P_r(x, j)$. From Equation (1), the channel DC gain can be stated as a

random variable with a normal distribution (in dB) about the distance-dependent mean. Thus, the value of $R_{\text{out},x}(i)$ is calculated using the Q-function:

$$Q(\alpha) = \frac{1}{\sqrt{2\pi}} \int_{\alpha}^{\infty} e^{-\frac{x^2}{2}} dx \qquad (27)$$

Therefore, we write

$$R_{\text{out},x}(i) = \int_{-\infty}^{\infty} Q\left(\frac{\bar{H}(x,i) - \frac{\sqrt{Out\_thr\left(ICI_{x,i}^2 + \sigma_{shot}^2 + \sigma_{thermal}^2\right)}}{\beta P_t}}{\sigma}\right) \cdot \frac{1}{\sqrt{2\pi}\sigma} e^{-\frac{G_o^2}{2\sigma^2}} dG_o, \qquad (28)$$

where $\bar{H}(x,i)$ is the average value of the channel DC gain when the user device is at location x.

The probability that the user device, whose current serving transmitter is transmitter i, does not need to utilize link switching at location x is defined as the probability that its received signal strength is not less than the LS_thr threshold. This probability, denoted as $R_{nls,x}(i)$, is calculated as

$$R_{nls,x}(i) = R(P_{\text{r}}(x,i) \geq LS\_thr) = R\left(H(x,i) \geq \frac{LS\_thr}{P_t}\right)$$

$$= \int_{-\infty}^{\infty} Q\left(\frac{\frac{LS\_thr}{P_t} - \bar{H}(x,i)}{\sigma}\right) \cdot \frac{1}{\sqrt{2\pi}\sigma} e^{-\frac{G_o^2}{2\sigma^2}} dG_o \qquad (29)$$

In the case that the user device needs to utilize link switching at location x and time t_{n+1}, the probability, denoted as $R_x(i, j)$, that it chooses the neighboring transmitter j as the next serving transmitter is expressed as

$$R_x(i,j) = R\big[\big(P_{r,pred}(j,t_{n+1}) \geq LS\_thr\big) \& \big(P_{r,pred}(j,t_{n+1}) > P_{r,pred}(k,t_{n+1})\big)$$
$$\& \big(P_{r,pred}(j,t_{n+1}) - P_r(j,t_n) > 0\big)\big] \qquad (30)$$

subject to $j \neq k, \forall j, k \in N_t$.

Equation (30) is derived as

$$R_x(i,j) = R\big[P_{r,pred}(j,t_{n+1}) \geq LS\_thr\big]$$
$$\times \prod_{k \neq j, \forall k, j \in N_t} R\big[P_{r,pred}(j,t_{n+1}) > P_{r,pred}(k,t_{n+1})\big]$$
$$\times R\big[P_{r,pred}(j,t_{n+1}) - P_r(j,t_n) > 0\big] \qquad (31)$$

To simplify the analysis, we assume that

$$R\big[P_{r,pred}(j,t_{n+1}) - P_r(j,t_n) > 0\big] = 1 \qquad (32)$$

and

$$P_{r,pred}(j,t_{n+1}) = \gamma P_r(x,j), \qquad (33)$$

where γ is the ratio that represents the mean relative accuracy of the prediction scheme ($\gamma > 0$). The value of γ is calculated as

$$\gamma = 1 - \frac{1}{M} \sum \frac{|P_{r,pred} - P_r|}{P_r}, \qquad (34)$$

where M is the total number of prediction samples.

Substituting Equations (32) and (33) into Equation (31), we have

$$R_x(i,j) = \int_{-\infty}^{\infty} R[\gamma P_r(x,j) \geq LS\_thr | G_\sigma = G_o]$$
$$\times \prod_{k \neq j, \forall k, j \in N_t} R[P_r(x,j) > P_r(x,k) | G_\sigma = G_o].R[G_\sigma = G_o] dG_o$$

$$= \int_{-\infty}^{\infty} Q\left(\frac{\frac{LS\_thr}{\gamma P_t} - \bar{H}(x,j)}{\sigma}\right) \cdot \prod_{k \neq j, \forall k, j \in N} Q\left(\frac{H(x,k) - \bar{H}(x,j)}{\sigma}\right)$$

$$\times \frac{1}{\sqrt{2\pi}\sigma} e^{-\frac{G_o^2}{2\sigma^2}} dG_o \qquad (35)$$

Equation (28) represents the outage probability of the user device, whose location and current serving transmitter are x and i, respectively, regardless of the link switching situation. If we consider the link switching situation, the outage probability of a conventional hard link switching scheme, denoted as $R_{out,x}^h(i)$, is expressed as

$$R_{out,x}^h(i) = R_{nlsw,x}(i)R_{out,x}(i) + \big(1 - R_{nls,x}(i)\big)$$
$$\times \big[\big(1 - R_D^h\big)R_x(i,j)R_{out,x}(j) + R_D^h R_x(i,j)R_{out,x}(i)\big], \qquad (36)$$

where R_D^h is the call dropping probability of a conventional hard link switching scheme.

To calculate the outage probability of a conventional soft link switching scheme, we need to take into account two connection links of the user device. This outage probability is calculated as

$$R_{out,x}^s(i) = R_{nlsw,x}(i)R_{out,x}(i) + \big(1 - R_{nls,x}(i)\big) \qquad (37)$$
$$\times \big[\big(1 - R_D^s\big)R_x(i,j)R_{out,x}(i)R_{out,x}(j)$$
$$+ R_D^s R_x(i,j)R_{out,x}(i)\big]$$

where $R_{out,x}^s(i)$ and R_D^s are the outage probability and the call dropping probability of a conventional soft link switching scheme, respectively.

Similar to the case of conventional soft link switching scheme, the outage probability of our proposed scheme represents the connections of the user device with its

current serving transmitter and the selected neighboring transmitter:

$$R_{out,x}^{prop}(i) = R_{nlsw,x}(i)R_{out,x}(i) + \left(1 - R_{nls,x}(i)\right) \qquad (38)$$
$$\times \left[(1 - R_D^{prop})R_x(i,j)R_{out,x}(i)R_{out,x}(j) \right.$$
$$\left. + R_D^{prop}R_x(i,j)R_{out,x}(i) \right],$$

where $R_{out,x}^{prop}(i)$ and R_D^{prop} are the outage probability and the call dropping probability of our proposed scheme, respectively.

3.2.3. Queuing analysis

To calculate the link switching call dropping probability, we use an M/M/K/K queuing model. We assume that the arrival and departure are Poisson processes. The states of this M/M/K/K queue represent the number of calls in the system. Let S and S_{req} be the total number of time slots in the system and the average number of required time slots for a call. We respectively denote λ_n and λ_h as the arrival rates of new calls and link switching calls. The relation between λ_n and λ_h is expressed by

$$\lambda_h = \frac{R_h(1 - R_B)}{[1 - R_h(1 - R_D)]}\lambda_n, \qquad (39)$$

where R_h, R_B, and R_D are the link switching probability of a call, the new call blocking probability, and the link switching call dropping probability, respectively.

The link switching probability of a call depends on two factors: the average channel dwell time ($1/\eta$) and the average call duration ($1/\mu$). Both the call duration and the cell dwell time are assumed to be exponential. R_h is calculated as

$$R_h = \frac{\eta}{\eta + \mu} \qquad (40)$$

Additionally, the time slot release rate is calculated as

$$\mu_r = \eta + \mu \qquad (41)$$

The average channel dwell time depends on the time a user device stays in the non-overlay area of transmitter i ($1/\chi$) and the time the user device stays in the overlay area between transmitter i and neighboring transmitter $i + 1$ ($1/p$). In the cases of the hard link switching scheme and our proposed scheme, this relation is expressed as

$$\frac{1}{\eta_h} = \frac{1}{\eta_{prop}} = \frac{1}{\chi} + \frac{1}{\rho} = \frac{\chi + \rho}{\chi\rho} \qquad (42)$$

In terms of the queuing model, there is no difference between our proposed scheme and the conventional hard link switching scheme. Figure 5 shows the Markov chain of the conventional hard link switching scheme

and our proposed scheme. The maximum number of states in the system, denoted as N, is calculated as

$$N = \frac{S}{S_{req}} \qquad (43)$$

By using the Erlang-B formula, the new call blocking probability and the link switching call dropping probability are calculated as

$$R_D^h = R_D^{prop} = R_B^h = R_B^{prop} = \frac{(\lambda_n + \lambda_h)^N}{N!(\mu_r)^N} \left[\sum_{i=0}^{N} \frac{(\lambda_n + \lambda_h)^i}{i!(\mu_r)^i} \right]^{-1} \qquad (44)$$

To support a soft link switching call, the system needs to use multiple channels simultaneously. Thus, the queuing model of the conventional soft link switching scheme is different from those of our proposed scheme and the conventional hard link switching scheme. Figure 6 shows the Markov chain of the conventional soft link switching scheme. We assume that a user device can connect with up to two transmitters during the soft link switching procedure. The average channel dwell time in this case is calculated as

$$\frac{1}{\eta_s} = \frac{1}{\chi} + \frac{1}{\rho} + \frac{1}{\rho} = \frac{2\chi + \rho}{\chi\rho} \qquad (45)$$

When the system is in state k ($0 \le k \le N$), the system resources (i.e., time slots) are released with rate $k(\mu + \eta_s)$. When the system is in state $N + j$ ($0 \le j < \infty$), all resources are used, and j link switching calls are looking for second links. If a new call arrives at state $N + j$, it is blocked immediately. Among all allocated calls, a completed call releases its resources with rate $N(\mu + \eta_s)$. For those j soft link switching calls, the calls leave the system if the user device leaves the overlay area (with rate ρ) or it is completed (with rate μ). Thus, the probability that the system is in state i ($0 \le i < \infty$) is expressed as

$$R(i) = \begin{cases} \dfrac{(\lambda_n + \lambda_h)^i}{i!(\mu + \eta_s)^i}R(0) & 0 < i \le N \\[2ex] \dfrac{(\lambda_n + \lambda_h)^N(\lambda_h)^{i-N}}{N!(\mu + \eta_s)^N \displaystyle\prod_{j=1}^{i-N}[N(\mu + \eta_s) + j(\mu + \rho)]}R(0) & N+1 \le i < \infty, \end{cases} \qquad (46)$$

where $R(0)$ is calculated from the normalizing condition $\sum_{n=0}^{\infty} R_n = 1$:

$$R(0) = \left[\sum_{i=0}^{N} \frac{(\lambda_n + \lambda_h)^i}{i!(\mu + \eta_s)^i} + \sum_{i=N+1}^{\infty} \frac{(\lambda_n + \lambda_h)^N(\lambda_h)^{i-N}}{N!(\mu + \eta_s)^N \displaystyle\prod_{j=1}^{i-N}[N(\mu + \eta_s) + j(\mu + \rho)]} \right]^{-1} \qquad (47)$$
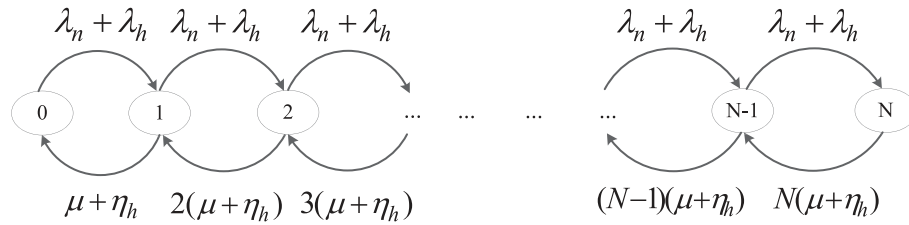
Figure 5 Markov chain of the conventional hard and proposed link switching schemes.

A new call is blocked if the system is in state i ($N \le i < \infty$). Thus, the new call blocking probability of the soft link switching scheme is expressed as

$$
\begin{aligned}
R_B^s &= \sum_{i=N}^{\infty} R(i) \\
&= \sum_{i=N}^{\infty} \frac{(\lambda_n + \lambda_h)^N (\lambda_h)^{i-N}}{(N-1)!(\mu + \eta_s)^{N-1} \prod_{j=0}^{i-N} [N(\mu + \eta_s) + j(\mu + \rho)]} R(0)
\end{aligned}
$$

(48)

A soft link switching call l is dropped in case that the system is in state i ($N \le i < \infty$), all existing link switching calls and at least one allocated call do not leave the system before call l leaves the overlay area. The soft link switching call dropping probability is calculated as

$$
\begin{aligned}
R_D^s = \sum_{j=0}^{\infty} \Bigg\{ 1 - \left(\frac{\mu + \rho}{N(\mu + \eta_s) + \mu + \rho} \right) \\
\times \prod_{n=1}^{j+1} \left[1 - \left(\frac{\mu + \rho}{N(\mu + \eta_s) + \mu + \rho} \right) \left(\frac{1}{2} \right)^n \right] \Bigg\} R(N+j)
\end{aligned}
$$

(49)

4. Performance evaluation

In this section, we evaluate the performance of our proposed link switching scheme by comparing it to conventional hard and soft link switching schemes. Several performance metrics are used for the comparison, including the link switching delay, unnecessary link switching ratio, new call blocking probability, link switching call dropping probability, and outage probability. We obtain both the simulated and numerical results to evaluate three link switching schemes. Table 1 shows the list of assumed parameters for the performance evaluation.

Regarding the simulation, we focused on building and analyzing the VLC MAC operation with a superframe structure, the conventional and proposed link switching procedures, and the channel path loss model that is shown in Equation (26). The transmitters we arranged in a room whose dimensions were fixed during the simulation. The distance between two adjacent transmitters was initially set to 3 m and was decreased when the number of transmitters used in the simulation was increased. In addition, in our simulation, the velocities of the user devices were equal and kept constant. To obtain objective results, the trajectories of the user devices were randomly arranged into various configurations, such as zigzag, arc line, straight line, etc.

Figure 7 shows a comparison of the average link switching delay among three schemes used in the simulation. In this experiment, the conventional hard link switching scheme has the worst performance. During the conventional soft link switching procedure, the connections between user devices and their serving transmitters are maintained, so the conventional soft link switching delay is zero regardless of the number of transmitters. By eliminating the scanning period, which is the main cause of the link switching delay, our proposed scheme effectively reduces the data transmission interruption. The link switching delay of our proposed scheme only suffers from a disassociation process between user devices and their current serving transmitters.

Figures 8 and 9 show the numerical results of the link switching call dropping probability and new call blocking
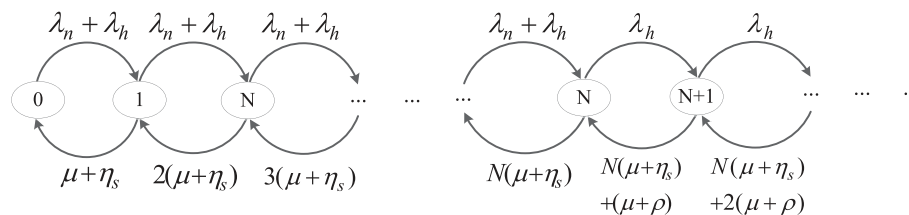

Figure 6 Markov chain of the conventional soft link switching scheme.

Table 1 Parameter assumptions

Parameter	Value
Photodetector area, A	0.9 cm^2
Signal transmission coefficient of optical filter, $T_S(\psi)$	1.0
Receiver FOV, Ψ_C	60°
Transmitter semi-angle at half power, $\varphi_{1/2}$	15°
Refractive index of optical concentrator, a	1.78
Transmitted power, P_t	30 mW
MacBeaconOrder, BO	9
MacSuperframeOrder, SO	8
ScanDuration, n	5
Number of channels, k	7
Path loss exponent, p	3
Scanning threshold, Scan_thr	−67 dBm
Association threshold, Assoc_thr	−80 dBm
Link switching threshold, LS_thr	−86 dBm
τ	3
Detector responsivity, β	0.53 A/W
Shot noise, σ^2_{shot}	0.031×10^{-18} A^2
Thermal noise, $\sigma^2_{\text{thermal}}$	8.2×10^{-16} A^2
SINR threshold, Out_thr	−92 dBm
Average non-overlay-staying time, $1/\chi$	10
Average overlay-staying time, $1/\rho$	3
Average call duration, $1/\mu$	80 s
Number of time slots, S	160
Average number of time slots required by a call, S_{req}	1
Velocity of user devices	0.5 m/s
Number of user devices	10
Room dimensions	25×25 m^2
Initial distance between two adjacent transmitters	3 m
MAC bit rate	10 Mbps

probability under various new call arrival rates. Our proposed scheme and the conventional hard link switching scheme achieve the same performance, whereas the conventional soft link switching scheme achieves the worst results among the three schemes. This result can be explained by the fact that because the conventional soft link switching scheme allocates more resources to a call (multiple transmitters serve a link switching call simultaneously), the system runs out of free resources faster than in the case of the two other schemes. Additionally, when the new call arrival rate increases, the link switching call dropping probability and the new call blocking probability also increases.

In the hard link switching case, the link switching delay is increased along with the increase in the number of transmitters in the system. The number of transmitters

also affects the unnecessary link switching ratio, as shown in Figure 10. The unnecessary link switching ratio is a parameter used to assess the performance of a link switching scheme in terms of coping with the ping-pong effect. The conventional hard and soft link switching schemes only choose the next serving transmitters for user devices based on the RSS values of neighboring transmitters at the selection time, so their unnecessary link switching ratios are equal. The simulation results shown in Figure 10 help in validating this assessment. Utilizing the knowledge of previous RSS values of neighboring transmitters combined with the RSS prediction scheme, our proposed scheme helps in choosing the next serving transmitters for user devices more precisely, so the unnecessary link switching ratio is decreased as well.

To deeply evaluate the performance of our proposed scheme compared to the conventional hard and soft link switching schemes, we apply a hysteresis margin-based method to the three schemes. In the hysteresis margin-based method, the best neighboring transmitter is chosen to be the next serving transmitter of a user device if its RSS value is larger than the RSS value of the current serving transmitter of the user device by a hysteresis margin. Using the hysteresis margin-based method, the values of the $R_{\text{nls},x}(i)$ and $R_x(i,j)$ probabilities are respectively modified as

$$R_{nls,x}^{hyst}(i) = R((P_{\text{r}}(x,i) \geq LS\_thr) \,|\, |(P_{r,pred}(j,t_{n+1}) - P_{\text{r}}(x,i) < Hys\_thr))$$

$$= \int_{-\infty}^{\infty} Q\left(\frac{\frac{LS\_thr}{P_t} - \bar{H}(x,i)}{\sigma}\right) \cdot \frac{1}{\sqrt{2\pi}\sigma} e^{-\frac{G_o^2}{2\sigma^2}} dG_o$$

$$+ \int_{-\infty}^{\infty} Q\left(\frac{\bar{H}(x,j) - \frac{Hys\_thr + P_{\text{r}}(x,i)}{\gamma P_t}}{\sigma}\right) \cdot \frac{1}{\sqrt{2\pi}\sigma} e^{-\frac{G_o^2}{2\sigma^2}} dG_o$$

$$(50)$$

and

$$R_x^{hyst}(i,j) = R[(P_{r,pred}(j,t_{n+1}) - P_r(x,i) \geq Hys\_thr)$$

$$\& (P_{r,pred}(j,t_{n+1}) > P_{r,pred}(k,t_{n+1}))$$

$$\& (P_{r,pred}(j,t_{n+1}) - P_r(j,t_n) > 0)]$$

$$= \int_{-\infty}^{\infty} Q\left(\frac{\frac{Hys\_thr + P_{\text{r}}(x,i)}{\gamma P_t} - \bar{H}(x,j)}{\sigma}\right)$$

$$\times \prod_{k \neq j, \forall k,j \in N_t} Q\left(\frac{H(x,k) - \bar{H}(x,j)}{\sigma}\right) \cdot \frac{1}{\sqrt{2\pi}\sigma} e^{-\frac{G_o^2}{2\sigma^2}} dG_o$$

$$(51)$$

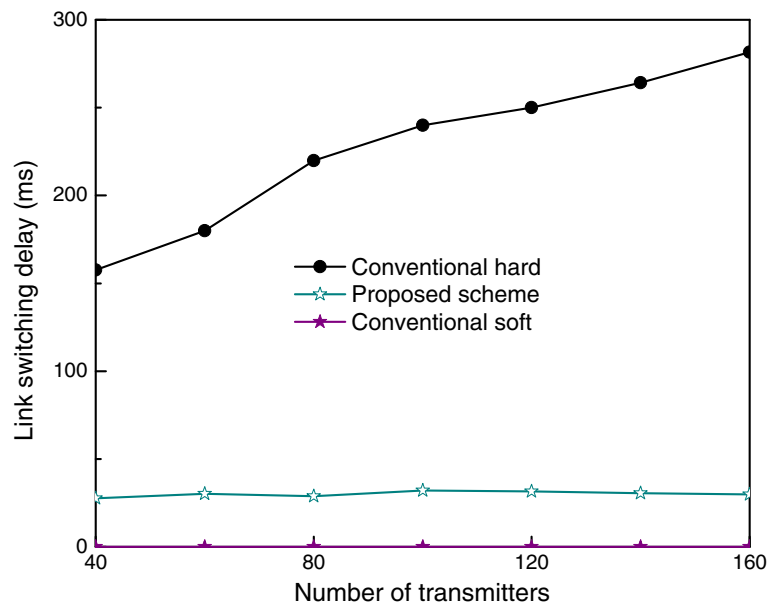where Hys_thr is a predefined value of the hysteresis margin.

Figure 7 Simulation results of the link switching delay versus number of transmitters.

The hysteresis margin method can help reduce the unnecessary link switching ratio that is validated by the simulation results shown in Figure 10 (the value of Hys_thr is set to 4 dB in our experiments). However, the use of a hysteresis margin results in an increase in the outage probability, which is made evident by the numerical results shown in Figures 11 and 12. In Figure 11, the outage probabilities of the three schemes according to the normalized distance are represented. In this experiment, the new call arrival rate is set to 1 call/s. In the region near the transmitters, where the normalized distance is less than or equal to 0.2, the outage probabilities of three schemes are almost equal to zero. The outage probability of our proposed scheme is lower than those of the two other schemes, even in the boundary area. In the cases of both using as well as not using the
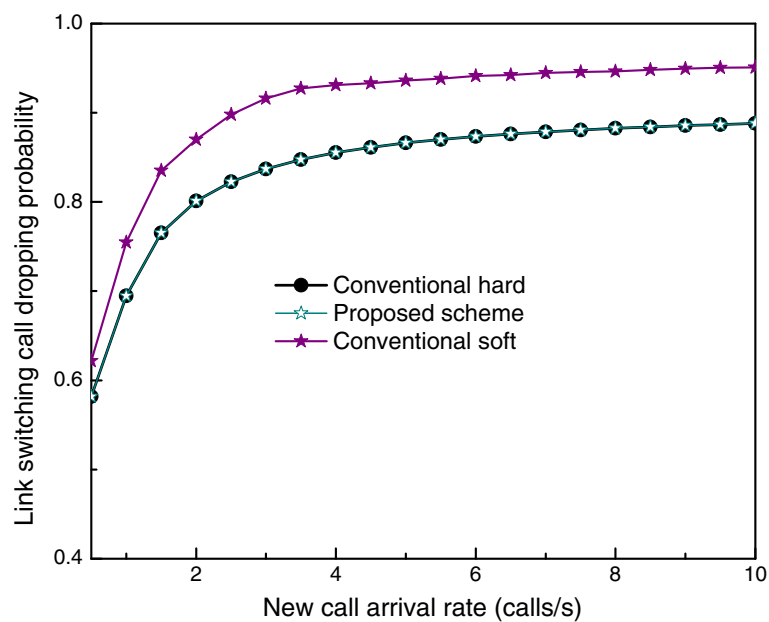
Figure 8 Numerical results of the link switching call dropping probability under various new call arrival rates.
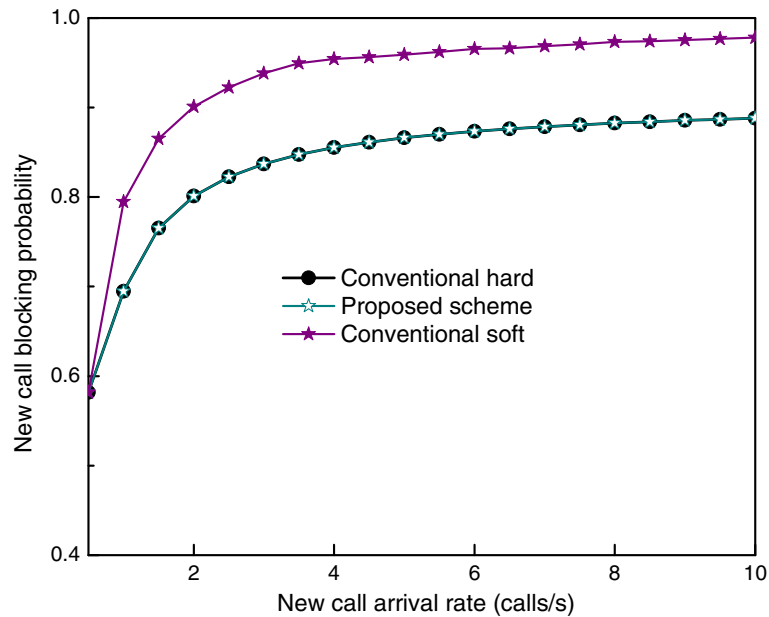
Figure 9 Numerical results of the new call blocking probability under various new call arrival rates.

hysteresis margin method, the conventional hard link switching scheme achieves the highest outage probability when the normalized distance is less than or equal to 0.8.

The new call arrival rate affects the link switching call dropping probability, so the outage probability is affected as well. Figure 12 shows the impact of the new call arrival rate on the outage probability when the normalized distance is equal to 0.5. The new call arrival rate affects the conventional soft link switching scheme more seriously than those two schemes. In the case when the hysteresis margin method is not used, when the new call arrival rate is less than or equal to 3 calls/s, the conventional hard link switching achieves the highest outage probability. However, when the new call arrival rate is higher than 3 calls/s,
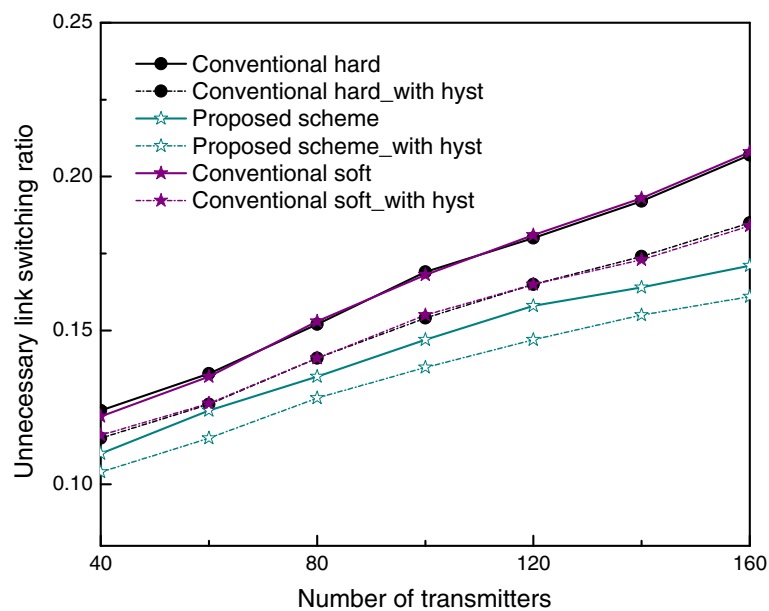

Figure 10 Comparison of the unnecessary link switching ratio using simulation results.
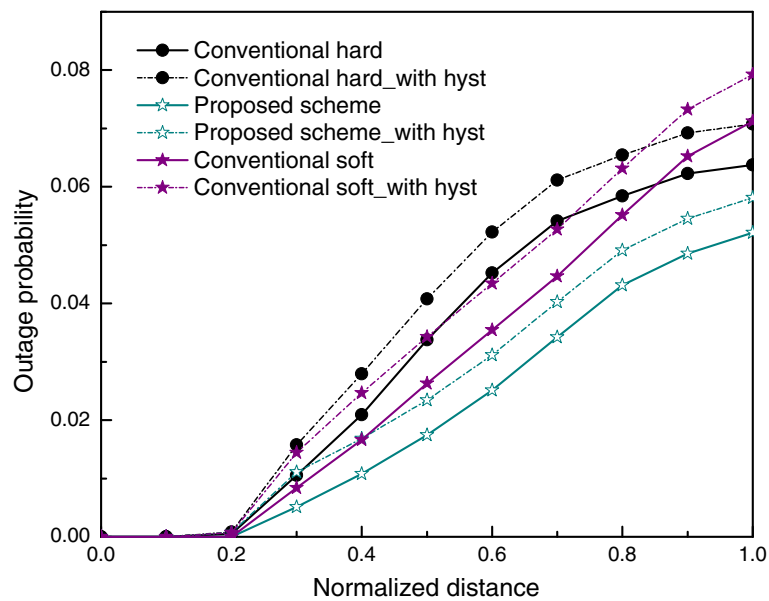
Figure 11 Numerical results of the outage probability according to normalized distance.

the outage probability of the conventional soft link switching scheme becomes the highest.

5. Conclusions

This paper has presented a novel hard link switching scheme, which overcomes the drawbacks of conventional hard and soft link switching schemes, for VLC networks. The proposed scheme uses pre-scanning and predictive RSS methods to reduce the link switching delay and the unnecessary link switching ratio. In addition, the SINR and the outage probability are analyzed with respect to the link switching situation in a VLC environment. The proposed scheme achieves a lower outage probability compared to the conventional hard and soft link switching schemes. To utilize our proposed scheme, there is no need to change the hardware of the user devices and
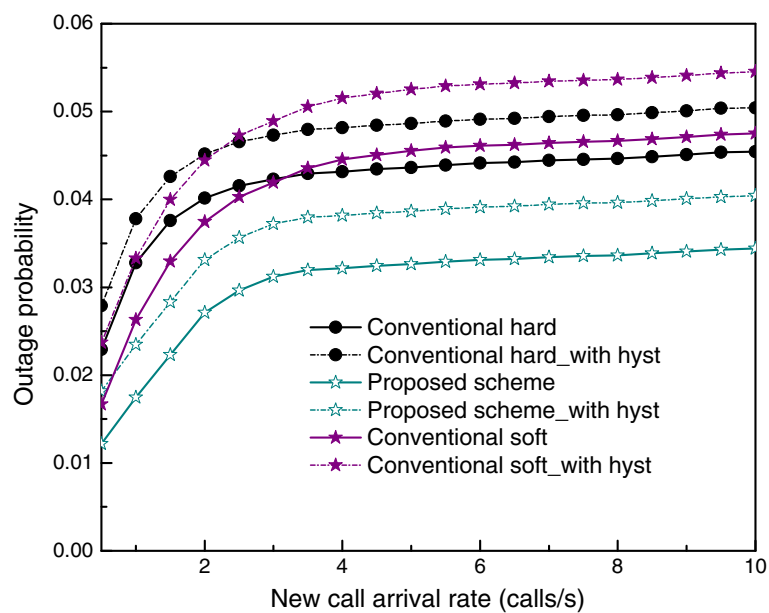

Figure 12 Numerical results of the outage probability under various new call arrival rates.

the IEEE 802.15.7 MAC operation. Therefore, the proposed scheme is expected to be a possible approach for a practical link switching implementation. In the future, we will work on handling the increase in the overhead caused by multiple pre-scannings in our proposed scheme.

Author details
[1]Department of Electronics Engineering, Kookmin University, Seoul 136-702, South Korea. [2]Department of Electrical and Electronic Engineering, Khulna University of Engineering and Technology, Khulna 9203, Bangladesh.

References
1. S Rajagopal, RD Roberts, SK Lim, IEEE 802.15.7 visible light communication: modulation schemes and dimming support. IEEE Commun. Mag. **50**(3), 72–82 (2012)
2. AM Khalid, G Cossu, R Corsini, M Presi, E Ciaramelia, Demonstrating a hybrid radio-over-fibre and visible light communication system. Electr. Lett. **47**(20), 1136–1137 (2011)
3. J Rufo, J Rabadan, FA Delgado, C Quintana, R Perez-Jimenez, Experimental evaluation of video transmission through LED illumination devices. IEEE Trans. Consum. Electr. **56**(3), 1411–1416 (2010)
4. AM Khalid, G Cossu, R Corsini, P Choudhury, E Ciaramella, 1-Gb/s transmission over a phosphorescent white LED by using rate-adaptive discrete multitone modulation. IEEE Photon. J. **4**(5), 1465–1473 (2012)
5. IEEE Standard, 802.15.7, *IEEE Standard for Local and Metropolitan Area Network– Part 15.7: Short-Range Wireless Optical Communication Using Visible Light* (IEEE Std, Piscataway, 2011)
6. H Lawrence, *Introduction to Mobile Telephone Systems* (ALTHOS, NC, 2006)
7. HP Lin, RT Juang, DB Lin, Validation of and improved location-based handover algorithm using GSM measurement data. IEEE Trans. Mobile Comput. **4**(5), 530–536 (2005)
8. IF Akyildiz, JSM Ho, M Ulema, Performance analysis of the anchor radio system handover method for personal access communications system, in *Proceedings of the IEEE International Conference on Computer Communications (INFOCOM)*. San Francisco, 24–28 March, 1996, pp. 1397–1404
9. K Uchida, J Honda, T Tamaki, M Takematsu, Handover simulation based on a two-rays ground reflection model, in *Proceedings of the International Conference on Complex, Intelligent and Software Intensive Systems (CISIS)*. Seoul, 30 June - 2 July, 2011, pp. 414–419
10. T Inzerilli, AM Vegni, A Neri, R Cusani, A location-based vertical handover algorithm for limitation of the ping-pong effect, in *Proceedings of the IEEE International Conference on Wireless and Mobile Computing, Networking and Communications (WIMOB'08)*. Avignon, 12–15 October, 2008, pp. 385–389
11. L Yun, L Man, C Bin, W Yong, L Wenjing, Dynamic optimization of handover parameters adjustment for conflict avoidance in long term evolution. China Commun. **10**(1), 56–71 (2013)
12. K Ghanem, H Alradwan, A Motermawy, A Ahmad, Reducing ping-pong handover effects in intra EUTRA networks, in *Proceedings of the 8th International Symposium on Communication Systems, Networks & Digital Signal Processing (CSNDSP)*. Poznan, Poland, 18–20 July, 2012, pp. 1–5
13. JH Lee, S Pack, T Kwon, Y Choi, Reducing handover delay by location management in mobile WiMAX multicast and broadcast services. IEEE Trans. Veh. Technol. **60**(2), 605–617 (2011)
14. JT Park, SM Chun, QoS-guaranteed IP mobility management for fast-moving vehicles with multiple network interfaces. IET Commun. **6**(15), 2287–2295 (2012)
15. M Gohar, SJ Koh, Network-based distributed mobility control in localized mobile LISP networks. IEEE Commun. Lett. **16**(1), 104–107 (2012)
16. AG Niteshkumar, KB Prasann, D Kaushal, V Agarwal, An advance approach to reduce handover delay by reducing scanning delay using media independent handover in 802.11, in *Proceedings of the International Conference on Computing Sciences (ICCS)*. Punjab, India, 14–15 September, 2012, pp. 159–162
17. D Lopez-Perez, I Guvenc, X Chu, Mobility management challenges in 3GPP heterogeneous networks. IEEE Commun. Mag. **50**(12), 70–78 (2012)
18. S Fernandes, A Karmouch, Vertical mobility management architectures in wireless networks: a comprehensive survey and future directions. IEEE Commun. Surv. Tut. **14**(1), 45–63 (2012)
19. TM Ali, M Saquid, Analytical framework for WLAN-cellular voice handover evaluation. IEEE Trans. Mobile Comput. **12**(3), 447–460 (2013)
20. J Bastos, M Albano, H Marques, J Ribeiro, J Rodriguez, C Verikoukis, Smart interface switching for energy efficient vertical handovers in ns-2. IET Commun. **6**(14), 2228–2238 (2012)
21. D Lopez-Perez, I Guvenc, X Chu, Theoretical analysis of handover failure and ping-pong rates for heterogeneous networks, in *Proceedings of the IEEE International Conference on Communications (ICC)*. Ottawa, 10–15 June, 2012, pp. 6774–6779
22. P Legg, G Hui, J Johansson, A simulation study of LTE intra-frequency handover performance, in *Proceedings of IEEE Vehicular Technology Conference Fall (VTC Fall)*. Ottawa, 6–9 September, 2010, pp. 1–5
23. A Roy, J Shin, N Saxena, Multi-objective handover in LTE macro/femto-cell networks. J. Commun. Networks. **14**(5), 578–587 (2012)
24. K Dimou, M Wang, M Kazmi, A Larmo, J Pettersson, W Muller, Y Timner, Handover within 3GPP LTE: design principles and performance, in *Proceedings of IEEE Vehicular Technology Conference Fall (VTC Fall)*. Anchorage, 20–23 September, 2009, pp. 1–5
25. MB Rahaim, AM Vegni, TDC Little, A hybrid radio frequency and broadcast visible light communication system, in *Proceedings of the IEEE GLOBECOM Workshops (GC Workshops)*. Houston, 5–9 December, 2011, pp. 792–796
26. AM Vegni, TDC Little, Handover in VLC systems with cooperating mobile devices, in *Proceedings of the International Conference on Computing, Networking and Communications (ICNC) 2012*. Maui, January 30 - February 2, 2012, pp. 126–130
27. T Nguyen, MZ Chowdhury, YM Jang, Flexible resource allocation scheme for link switching support in visible light communication networks, in *Proceedings of International Conference on ICT Convergence (ICTC)*. Jeju, 15–17 October, 2012, pp. 145–148
28. IEEE Standard 802.15.4, *IEEE Standard for Local and Metropolitan Area Networks – Part 15.4: Low-Rate Wireless Personal Area Network (LR-WPANs)* (IEEE Std, Piscataway, 2011)
29. BJ Chang, JF Chen, Cross-layer-based adaptive vertical handoff with predictive RSS in heterogeneous wireless networks. IEEE Trans. Veh. Technol. **57**(6), 3679–3692 (2008)
30. J Kiusalaas, *Numerical Methods in Engineering with Python* (Cambridge University Press, New York, 2005)
31. JM Kahn, JR Barry, Wireless infrared communications. Proc. IEEE **85**(2), 265–298 (1997)
32. S Dimitrov, R Mesleh, H Haas, M Cappitelli, M Olbert, E Bassow, On the SIR of a cellular infrared optical wireless system for an aircraft. IEEE J Sel. Area Commun. **27**(9), 1623–1639 (2009)